

Article

Experimental Proof-of-Concept of a Hybrid Wave Energy Converter Based on Oscillating Water Column and Overtopping Mechanisms

Irene Simonetti ^{1,*}, Andrea Esposito ² and Lorenzo Cappiotti ¹¹ Department of Civil and Environmental Engineering, Università degli Studi di Firenze, 50139 Florence, Italy² AM3 Spin-Off, Joint Laboratory A-MARE, 50139 Florence, Italy

* Correspondence: irene.simonetti@unifi.it

Abstract: This paper presents the results of laboratory tests on a hybrid wave energy converter concept, the O²WC (Oscillating-Overtopping Water Column) device. The proposed device aims at providing an alternative to the classical OWC concept, storing part of the wave energy of the highly energetic sea states in a second chamber at atmospheric pressure, through overtopping phenomena. In this way, the maximum airflow rate and air pressure in the OWC chamber are reduced, possibly aiding the safe functioning of the air turbine, and allowing to exploit the excess of energy instead of dissipating it through by-pass valves. The performance of the device is investigated under different incident wave conditions, for different design parameters. The height of the overtopping threshold from the second chamber of the device which allows to maximize the performance has been selected. Results show that the decrease of the primary conversion efficiency of the OWC component of the device caused by the decreased air pressure in the OWC chamber can be partially compensated by the additional energy stored in the overtopping chamber of the O²WC device. Overall, the studied O²WC device has capture width ratio values ranging between 0.3 and 0.7.

Keywords: oscillating water column; overtopping devices; hybrid wave energy converters; laboratory tests; proof-of-concept; breakwater integrated



Citation: Simonetti, I.; Esposito, A.; Cappiotti, L. Experimental Proof-of-Concept of a Hybrid Wave Energy Converter Based on Oscillating Water Column and Overtopping Mechanisms. *Energies* **2022**, *15*, 8065. <https://doi.org/10.3390/en15218065>

Academic Editors: Kostas Belibassakis, Eugen Rusu and George Lavidas

Received: 3 October 2022

Accepted: 25 October 2022

Published: 30 October 2022

Publisher's Note: MDPI stays neutral with regard to jurisdictional claims in published maps and institutional affiliations.



Copyright: © 2022 by the authors. Licensee MDPI, Basel, Switzerland. This article is an open access article distributed under the terms and conditions of the Creative Commons Attribution (CC BY) license (<https://creativecommons.org/licenses/by/4.0/>).

1. Introduction

Wave Energy Conversion (WEC) technologies have the recognized potential to contribute to the global renewable energy market. Despite the conspicuous investments in research activities received during the last decades and the extensive efforts of researchers and developers, the wave energy conversion sector has still not reached commercial maturity [1]. Among the different technical and non-technical barriers to the broader technology diffusion of WECs [2], the reduction of costs and the increase in reliability have been identified as the main challenges [3]. The Levelized Cost Of Energy (LCOE) of WEC is at present estimated as ranging between 90–100 €/MWh for onshore applications and 180–490 €/MWh for offshore technologies. Comparing these values with wind energy (up to 100 €/MWh in the offshore case), or solar photovoltaic (~68 €/MWh), it is apparent that the wave energy is not currently cost-effective [4,5].

Over the years, several WEC technologies have been specifically studied and developed to match the Mediterranean wave climates (e.g., [6–10]). Such previous studies highlighted in particular that devices designed for more energetic sea states need to be properly downscaled to be cost-effective.

Hybrid WECs, combining two or more concepts for wave energy conversion, have been recently proposed as a possible strategy to operate the devices in synergy with satisfactory performance (e.g., [11–13]). Such synergy could, from one side, increase the overall wave energy conversion performance of the device and, from the other side, lower

its specific CAPEX by sharing part of the structure among two or more different technologies, thus contributing to lower the overall LCOE.

The Oscillating Water Column (OWC) is one of the more consolidated WEC concepts, as thoroughly reviewed e.g., by Falcão & Henriques [14]. A column of water, in a partially submerged structure, oscillates under the excitation of the external wave motion, compressing and decompressing an above-standing air pocket constrained in a chamber and creating an alternating airflow through a duct. This pneumatic energy is then converted into mechanical energy by an air turbine and finally into electrical energy by an electrical generator. In recent years, vast research effort has been devoted to the optimization of OWCs to maximize the wave energy conversion performance. It has been proved that this WEC can attain primary conversion efficiencies (i.e., from the wave energy to the pneumatic energy in the airflow in/out the OWC chamber) between 70 and 90% under specific wave conditions [15–17], generally decreasing to values between 30 and 60% when considering average performance over all the sea states that characterize specific installation sites (e.g., [18,19]). Despite the relatively high diffusion of the concept, the OWC technology has some drawbacks, e.g., it has limited operability in highly energetic sea-states, due to the sudden loss of efficiency induced by stall phenomena or to the possible damages at the air turbine caused by green water jets reaching it or excessive centrifugal stresses and shock waves in the more energetic sea states [20,21]. To overcome this problem, systems of relief (or by-pass) valves have been proposed [22–25]. Relief valves are opened when the pressure in the air chamber exceeds a certain limit (which is strongly turbine-specific), therefore the excess of wave energy is passively dissipated. Moreover, the functioning of such valve systems may be negatively affected by the marine environment, which may in practice limit its lifetime due to corrosion and/or biofouling issues.

A different, well-established, WEC is the so-called OverTopping Device (OTD). In OTD devices, water volumes due to wave overtopping are stored in a reservoir, located above the Still Water Level (SWL), which may be floating [26] or fixed [27]. In this way, the wave energy is accumulated in the form of potential energy and then converted into mechanical energy through low-head hydraulic turbines and into electrical energy in an electrical generator (Power Take Off, PTO system). OTDs have some recognized advantages, e.g.: (i) the intermittently available wave energy can be stored in the form of potential energy; (ii) the low-head hydraulic turbine used as PTO is a well-consolidated technology, with a rather high energy conversion efficiency. Nevertheless, wave overtopping is, by its own nature, a threshold process, taking place only for relatively high energetic sea states, limiting the fraction of the total incident wave energy which can effectively be converted in the device. For OTD, primary conversion efficiencies (i.e., from the wave energy to the potential energy stored in the reservoir) between 10 and 30% are documented in the literature [12,28].

Both the aforementioned OWC and OTD WEC technologies are particularly suited for integration into harbour breakwaters, as demonstrated by the OWC prototype-scale installations in Mutiku (Spain) [29], the REWEC3 OWC in Civitavecchia (Italy) [30] and the OBREC OTD in Naples (Italy) [31–33]. The integration of WEC in maritime structures offers a further possibility to lower the CAPEX of WECs by sharing construction costs with the harbour structure while adding the extra benefit of renewable energy conversion. For breakwater-integrated OTDs, the increase in construction costs due to the presence of the WEC, compared to a traditional breakwater, has been quantified in the order of 10% [34].

In this context, the O²WC (Oscillating-OverTopping Water Column device), a hybrid WEC based on OWC and OTD technologies originally proposed by Cappiotti et al. [11], is under further development at A-MARE laboratory of Florence University, a joint laboratory participated by private companies. The O²WC device aims at providing an upgrade of the classical OWC concept, allowing to store the non-exploitable energy in highly energetic sea states (i.e., the fraction of energy that would be dissipated by relief-valves at very high pressures in a conventional OWC) in a second chamber at atmospheric pressure by exploiting wave overtopping phenomenon to feed an OTD device.

This study presents the results of a laboratory test campaign on a 1:25 scaled model of the hybrid O^2WC wave energy converter. The performance (in terms of primary conversion efficiency or capture width ratio) and the suitability of the concept to both extract the wave energy and reduce the maximum air pressure in the primary OWC chamber under the highly energetic wave conditions (thus contributing to safer operability of air turbine) are evaluated and discussed.

The paper is structured as follows: the O^2WC concept and the previous studies carried out are briefly presented, and then an overview of the new laboratory test campaign is given, with a focus on the methodology for data analysis (Section 2). Results are later presented and discussed in Sections 3 and 4, respectively. Conclusions are given in Section 5.

2. Materials and Methods

2.1. The O^2WC Concept and the Previous Preliminary Studies

The hybrid O^2WC -WEC concept basically consists of two chambers, each containing an inner water column which oscillates under the action of the incident wave motion (Figure 1). The first chamber (referred to, hereafter, as the OWC chamber) closely resembles a conventional OWC device: the air pressure difference between the inner chamber and the exterior induces an airflow, which activates an air turbine constituting the PTO system. In the O^2WC , the OWC chamber is hydraulically connected to the second chamber (referred to, hereafter, as the OTD chamber) through a submerged aperture located on its back wall. The internal free surface in the OTD chamber is constantly subjected to atmospheric pressure (i.e., the chamber has no roof). When the level of the free surface in the OTD chamber exceeds the level of its back wall, overtopping water flows are accumulated into a reservoir, located above the SWL. The potential energy of the water stored in the reservoir can be converted by using a low-head hydraulic turbine.

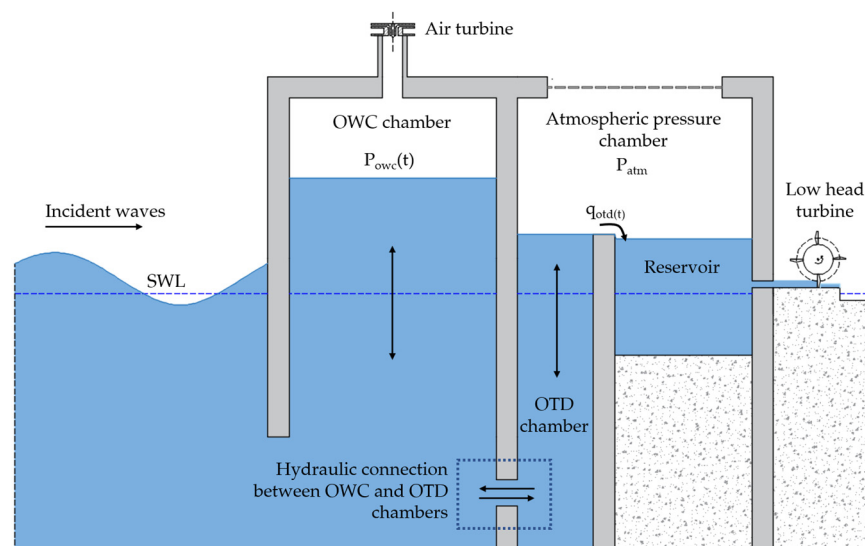


Figure 1. Sketch of the functioning of the O^2WC hybrid device.

The O^2WC device, particularly suitable for harbour breakwater integration, has been designed with the dual objective of (i) limiting the maximum air pressure and airflow rate into the OWC chamber, aiding to avoid possible damage to the turbine in highly energetic sea states and (ii) storing this excess of energy in the form of potential energy to be used when more needed (as conventionally done in OTDs).

The conceptual design of the O^2WC differs from the previously proposed hybrid devices combining OWC and OTD principles (e.g., [12,13,35,36]) since in the O^2WC the OWC and OTD chambers have a direct hydraulic connection through the underwater aperture that allows limiting the air pressure in the OWC chamber. A first set of laboratory tests on the O^2WC device were performed in the wave-current flume of LABIMA at

Florence University, Italy, in 2015 as documented in [11]. These laboratory tests allowed us to preliminarily assess the feasibility of the concept and estimate its primary wave energy harvesting efficiency. Preliminary results suggested that the O²WC device could have fairly promising performances, showing: (i) the effectiveness of the proposed concept in limiting the pressure in the OWC chamber, (ii) a primary efficiency of the OWC chamber reaching a maximum value of around 0.6 and (iii) efficiency of the OTD component lower than 0.02 in all the tested configurations. In the previous laboratory tests, the set of design parameters, only tentatively proposed, was left unchanged, without any attempt towards optimization of the design of the O²WC. Moreover, the tested model was affected by three-dimensional effects, limiting the possibility of using such an experimental database to validate two-dimensional numerical models (useful to further study the concept with more affordable computational cost than three-dimensional approaches).

Therefore, the new experimental test campaign documented in the present work has been conducted, aiming at more deeply analysing the hydraulic performance of the proposed O²WC concept. The new model has been designed to be fully two-dimensional, allowing a more consistent comparison with the results of two-dimensional numerical simulations.

2.2. The Small-Scale Laboratory Model of the O²WC

The O²WC model has been designed and tested according to Froude similarity, with a representative scale ratio 1:25 (Figure 2). The model has a width transversal to wave propagation direction corresponding to that of LABIMA wave flume (i.e., $B = 0.79$ m, maintaining a 5 mm tolerance at both sides), to impose a fully two-dimensional wave structure interaction. An overview of the design parameters of the model is provided in Table 1.

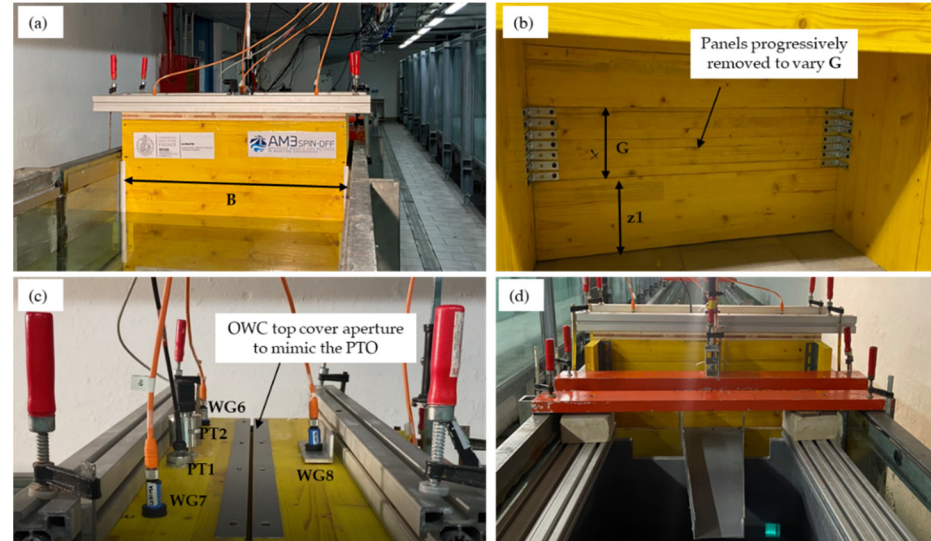


Figure 2. The 1:25 scaled model of the O²WC installed in LABIMA wave-current flume (a); detail of the OWC chamber back wall, with the different panels used to vary the size of the submerged opening G during the tests (b); the sensors installed on the top cover of the OWC chamber (WG: wave gauge, PT: pressure transducer) and the slot mimicking the PTO pressure drop (c); detail of the overtopping collecting ramp installed in the OTD chamber (d).

Table 1. Parameters of the O²WC model (values at laboratory scale 1:25).

Symbol	Description	Value	Units
B	Width of the O ² WC model perpendicular to the wave direction	0.79	[m]
D	Draft of the OWC chamber	0.20	[m]
Fb	Freeboard of the OWC chamber	0.3	[m]
G	Gap in the OWC back wall	0–0.12	[m]
$ht1, ht2, ht3$	Height of the overtopping threshold in the second chamber	0.61–0.65	[m]
h	Water depth	0.59	[m]
W	Width of the OWC chamber in the wave propagation direction	0.33	[m]
$W2$	Width of the overtopping chamber in the wave propagation direction	0.088	[m]
Wf	Width of the aperture on the top cover of the OWC chamber used to mimic the pressure drop	5	[mm]
$z1$	Distance of the gap in the OWC back wall from the bottom	0.14	[m]

The draft ($D = 0.2$ m) and the width in wave propagation direction ($W = 0.33$ m) of the OWC chamber were kept fixed during the tests, with values chosen based on the results of specific optimization studies previously performed on conventional OWC devices (e.g., [17]). With the adopted value of W , the relative OWC chamber width W/L (being L the wavelength of the tested incident waves) varies between 0.068 and 0.215. Based on the previous studies, the considered range of W/L -values contains the optimal working condition to maximize the wave energy extraction performance of a conventional OWC chamber (indeed, the best performance was obtained for $W/L \approx 0.12$ [17]). The draft D of the OWC chamber has been fixed to avoid the phenomena of inlet broaching for the target wave conditions (Section 2.3). The width of the OTD chamber is fixed to a value of $W2 = 8.8$ cm. The working water depth in the wave flume is $h = 0.59$ m.

To test a fully two-dimensional model, the turbine-induced damping is introduced in the laboratory model by using a slot, extending along the full width of the OWC chamber, having a width of $Wf = 5$ mm. The area of the slot corresponds to 1.6% of the area of the top cover of the OWC chamber (a value which was found to guarantee appreciable wave energy extraction performance in previous studies, e.g., in [17,37]). Using orifices, or slots as in the present two-dimensional study, to mimic the PTO damping in laboratory scale models of OWC devices is a consolidated experimental technique, regularly applied since the first documented studies in the literature (e.g., [38]) to the most recent ones (e.g., [39]). Indeed, relevant scale effects would make it unfeasible to adequately reproduce the air turbine at the model scale used in most of the available experimental facilities [14].

The submerged opening connecting the OWC and the OTD chambers extends along the full width of the model, to preserve the two-dimensional geometry. The submerged opening is located at a fixed distance from the bottom, $z1 = 0.14$ m (Figure 2b) and has a variable size ($G = 0$ –12 cm, with a step of 2 cm). To vary the size of the opening, the rear wall of the OWC chamber was manufactured as the union of several panels (Figure 2b), having a height of 2 cm each, screwed to the side walls of the model with L-shaped brackets in order to be easily removed during the tests. The joints of the panels have been sealed with silicone to guarantee watertight integrity. When varying G , panels were progressively removed starting from the lower ones, i.e., an increase of G also means decreasing the depth at which the aperture is located.

Different values of the overtopping threshold in the second chamber ht ($ht = 0.61, 0.63, 0.65$ cm) were tested as well. The model is entirely manufactured in plywood panels, having a thickness of 27 mm.

2.3. Test Conditions and Wave Generation

Aiming to assess the feasibility of the O²WC concept to both (i) extract the incident wave energy from the design wave conditions and (ii) reduce the maximum pressure in the air chamber in highly energetic wave conditions, waves with heights varying between 0.08 and 0.16 m (2 and 4 m at full scale) have been tested, with periods in the range 1–2 s (5–10 s at full scale). Values of wave steepness H/L in the range 0.018–0.078 are therefore considered.

The O²WC model has been preliminarily tested in regular waves only. The tested wave conditions at model scale 1:25 are reported in Table 2. A piston-type wave maker was used in the wave flume to generate the waves, by using a second-order generation algorithm. Twenty wave periods long tests ($20 \cdot T$) were performed, with two additional $4 \cdot T$ long linear ramps at the beginning and at the end of wave generation. The duration of each test was chosen to guarantee an analysis time window free from the presence of the waves which would be reflected towards the model by the wave maker paddle. Overall, 290 tests were performed, combining the different model configurations and wave conditions studied.

Table 2. Regular wave conditions tested (values at laboratory scale 1:25).

Wave Code	H [m]	T [s]	L [m]	H/L [-]	Wave Code	H [m]	T [s]	L [m]	H/L [-]
H01	0.08	1	1.54	0.052	H10	0.12	1.6	3.25	0.037
H02	0.08	1.2	2.12	0.038	H11	0.12	1.8	3.79	0.032
H03	0.08	1.4	2.33	0.034	H12	0.12	2	4.33	0.028
H04	0.08	1.6	3.25	0.025	H13	0.16	1.2	2.12	0.075
H05	0.08	1.8	3.79	0.021	H14	0.16	1.4	2.33	0.069
H06	0.08	2	4.33	0.018	H15	0.16	1.6	3.25	0.049
H07	0.12	1	1.54	0.078	H16	0.16	1.8	3.79	0.042
H08	0.12	1.2	2.12	0.057	H17	0.16	2	4.33	0.037
H09	0.12	1.4	2.33	0.052					

2.4. Experimental Set-Up of the Wave Flume

The O²WC model was located 32.47 m far from the wave maker (Figure 3). Nine ultrasonic distance sensors (Wave Gauges, WG1–WG9, Figure 3) were used to measure the level of the free surface in the wave flume and inside the chambers of the model. The WGs have an accuracy of ± 1 mm at a distance from the sensor in the range 60–500 mm.

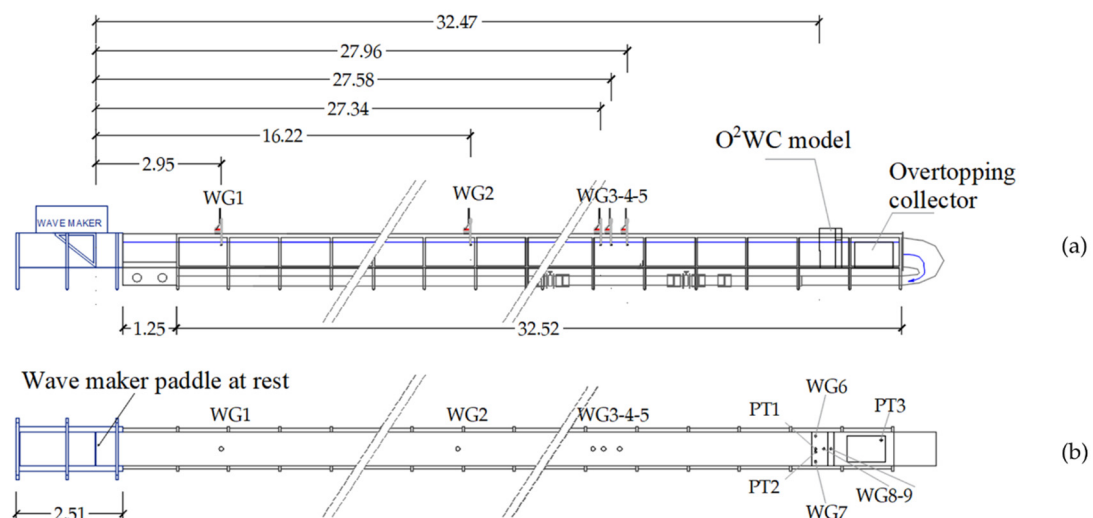


Figure 3. Position of the O²WC model and sensors installed the wave-current flume: longitudinal cross-section view (a) and top view (b). WG: ultrasonic wave gauge; PT: pressure transducer.

The incident waves were characterized based on measurements of gauges WG3–WG5, that were positioned in front of the model. Additional measurements at WG1 and WG2 were used to monitor the wave dissipation along the wave flume. The dissipation of the incident waves from WG3–WG5 position to the model was confirmed to be negligibly small.

WG6, WG7 and WG8 were used to sample the water level inside the OWC chamber, collecting redundant measurements of the same quantity to check whether the hypothesis of flat heave motion of the free surface inside the OWC chamber, needed for the subsequent data analysis, was consistent. WG9 is used to measure the free surface oscillation in the overtopping chamber. Two differential Pressure Transducers (PT1 and PT2, with a Full-Scale range FS of 100 mBar and 30 mBar, respectively, and accuracy of $\pm 0.1\%$ FS) have been used to measure the air pressure variations in the OWC chamber.

The volume of water overtopping from the OTD chamber into the reservoir has been measured by collecting the water flowing over the level of the back wall of the second chamber (Figure 2d). The mean overtopping discharge rate q_{otd} was determined by measuring the water level variation inside the reservoir during each test, using a pressure transducer (PT3). For all the sensors, the signal was acquired at a 200 Hz frequency.

2.5. Data Analysis

The overall primary capture width ratio of the O²WC device, CW , can be expressed as the ratio of the incident wave power per unit width P_{wave} [W/m] to the power comprehensively extracted by the device. The period averaged incident wave power per unit width P_{wave} [W/m] is computed as in Equation (1):

$$P_{wave} = \frac{1}{16} \rho g H^2 \frac{\omega}{k} \left(1 + \frac{2kh}{\sinh(2kh)} \right) \quad (1)$$

where ρ is the water density, H is the height of the incident, regular, wave, ω is the wave frequency, k is the wave number and h is the water depth.

The power extracted by the device is given by the sum of two contributions: (i) the pneumatic power of the air flux through the top cover slot in the OWC chamber, P_{owc} , available to be extracted with an air turbine; (ii) the hydraulic power of the water flow overtopped from the OTD chamber, stored into a reservoir and available to be extracted by a low-head turbine, P_{otd} .

Under the hypothesis of air incompressibility and that of flat rigid-piston-like heave motion of the free surface inside the OWC chamber, the mean pneumatic power absorbed by the OWC, P_{owc} [W], is estimated by integrating over the duration of the records, T_{test} , the product of the differential pressure of the air measured in OWC chamber, $p(t)$, the water surface level variation in the same chamber $d\eta_{owc}/dt$ and the cross-sectional area of the OWC, A_w

$$P_{owc} = \frac{1}{T_{test}} \int_0^{T_{test}} p(t) \cdot \frac{d\eta_{owc}}{dt} \cdot A_w dt \quad (2)$$

It is worth mentioning that the air incompressibility hypothesis introduces approximations in the estimation of the performance of OWC devices at full scale, as quantified in several previous studies in the literature [40–43]. This aspect is not addressed in the present work.

In the OTD chamber, the hydraulic power available to be converted by the low-head hydraulic turbine, P_{otd} [W], can be estimated as:

$$P_{otd} = q_{otd} \cdot \Delta h_{otd} \cdot \rho \cdot g \quad (3)$$

where q_{otd} is the average flow discharge from the overtopping chamber and g is the gravitational acceleration. Δh_{otd} is assumed to be fixed and determined as the difference between the SWL and the height of the overtopping threshold from the OTD chamber, h_t . The

overall capture width ratio (or primary conversion efficiency) of the O²WC device can be expressed as:

$$CW = CW_I + CW_{II} = \frac{P_{owc}}{P_{wave} \cdot B} + \frac{P_{otd}}{P_{wave} \cdot B} \quad (4)$$

It is worth pointing out a specific methodological aspect of the laboratory tests performed in the present work to assess CW_I . As mentioned in Section 2.4, redundant measurements of the free surface oscillation were taken to monitor the validity of the assumption of flat heave motion of the inner water surface inside the OWC chamber. As a preliminary way to quantify the possible impact of deviations from such a hypothesis on the quantity of interest, the values of CW_I obtained based on the water level measurements η_{owc} recorded at different WGs were compared to that obtained using the average of η_{owc} measurements from WG6, WG7 and WG8 (Figure 4).

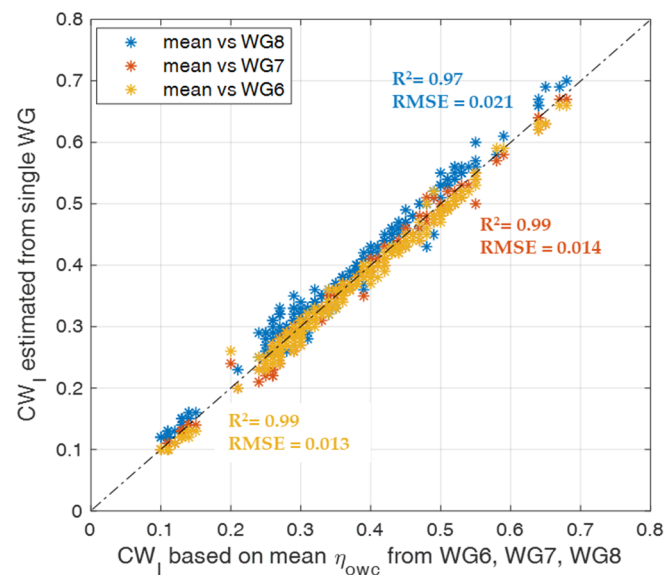


Figure 4. Capture width of the OWC chamber, CW_I , estimated with the free surface level η_{owc} obtained as the average of measurements at WG6, WG7 and WG8 vs. direct estimation of CW_I based on measurements from a single WG: WG6 (yellow), WG7 (orange) and WG8 (blue).

Results proved that the differences in the estimated value of CW_I are acceptably small for the purposes of the present study, with Root Mean Square Error (RMSE) of 0.013–0.021 when comparing CW_I estimated from the average of records at the different WG inside the OWC chambers and that obtained using WG6, WG7 or WG8 only, respectively. Hereafter, CW_I values based on average water level measurements from the available WGs will be presented.

3. Results

The effect of the different geometrical parameters and wave conditions on the capture width of the O²WC device is presented in this section, analyzing separately the two contributions of the OWC-based and OTD-based components of the hybrid device (Section 3.1). The capability of the O²WC concept to limit the maximum air pressure in the OWC chamber is later assessed (Section 3.2).

3.1. Capture Width Ratio of the Device

3.1.1. Effect of the Size of the Submerged Aperture Connecting the Two Chambers G/H

The performance of the OWC-based component of the device, expressed in terms of capture width CW_I , as a function of the size of the underwater aperture connecting the OWC and the OTD chambers relative to the incident wave height, G/H , is reported in Figure 5.

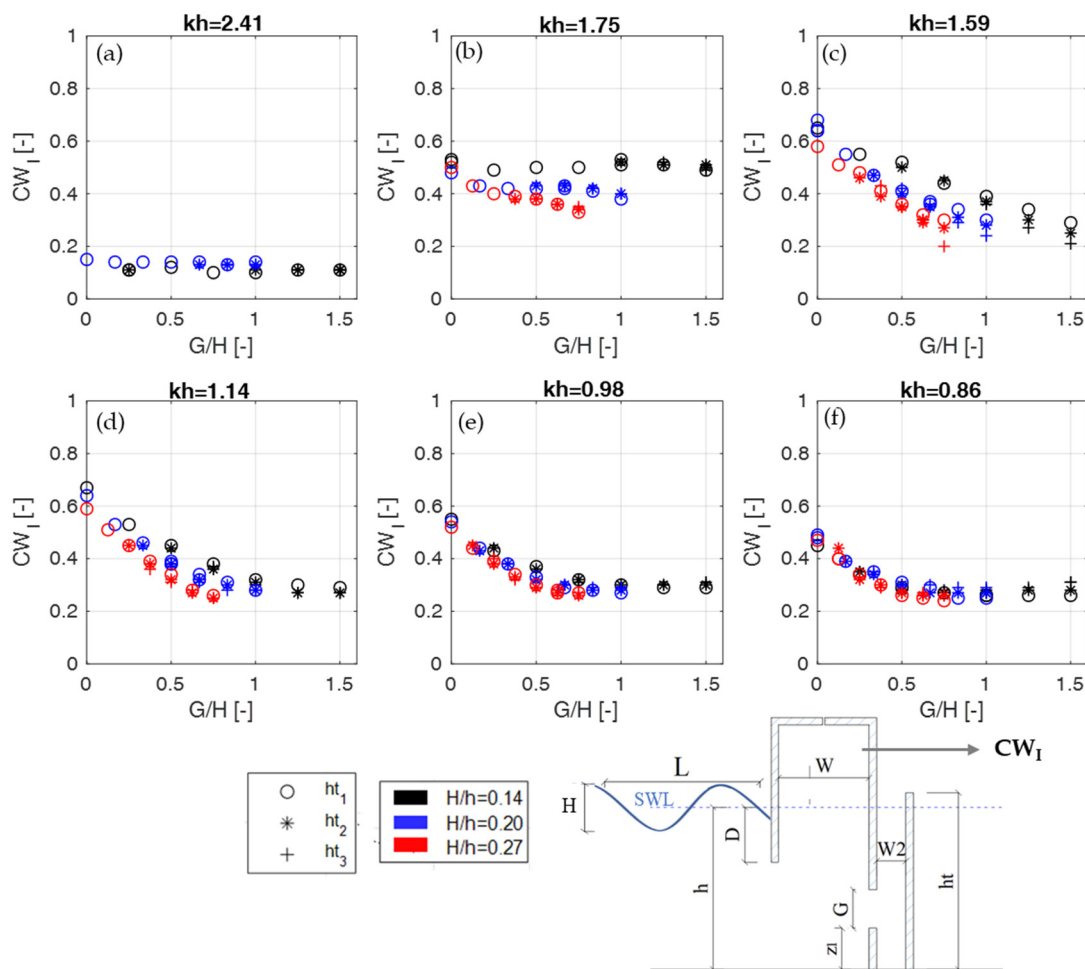


Figure 5. Capture width of the OWC chamber CW_I as a function of the relative size of the submerged aperture G/H for different relative water depths: $kh = 2.41$ (a), 1.75 (b), 1.59 (c), 1.14 (d), 0.98 (e), 0.86 (f).

For the higher values of relative water depth tested (i.e., $kh = 2.41$ and $kh = 1.75$, Figure 5a,b), CW_I is relatively insensitive to G/H . Such a result can be easily interpreted considering that for the higher kh -values (i.e., for the shorter waves on a fixed water depth h) the submerged connection is located at a depth where the dynamics and kinematic effects associated with the surface wave motion are negligible. For $kh = 2.41$, CW_I has an almost constant value between 0.13 and 0.18. For $kh = 1.75$, CW_I varies between 0.35 and 0.55, again with negligible dependence on G/H but showing, instead, an evident dependence on the relative incident wave height H/h : higher efficiency values are obtained for the smallest incident wave $H/h = 0.14$. Increasing the wave height, CW_I decreases up to 20 percentage points (Figure 5b), possibly due to the higher losses taking place for higher and steeper waves.

For relative water depths $kh < 1.75$ (Figure 5c–f), the capture width of the OWC chamber CW_I significantly decreases when increasing the size of the submerged opening G/H . For $kh = 1.59$, CW_I has a maximum of around 0.7 for $G/H = 0$ (i.e., for the configuration resembling a classical OWC, with a completely closed back wall), which decreases to values close to 0.2 for $G/H = 1.5$. The observed decreasing trend is almost linear, with a higher rate of decrease for the higher relative incident wave heights H/h (Figure 5c).

Further increasing the relative water depth, the range of G/H -values for which an approximately linear decreasing trend of CW_I with G/H is observed becomes progressively narrower: for $kh = 1.14$ (Figure 5d), CW_I decreases between $0 < G/H < 1$, while further decreasing G/H has no remarkable effect on the capture width. For $kh = 0.98$ and

$kh = 0.86$, CW_I remains approximately constant for values of G/H greater than 0.75 and 0.5, respectively (Figure 5e,f).

It is also worth pointing out that the effect of different relative wave heights H/h on CW_I becomes progressively less significant when decreasing the relative water depth kh . Therefore, nonlinear effects associated with increasing the wave heights seem to be more related to the wave steepness than to the asymmetry of the wave profile induced by wave-bottom interaction. Moreover, the height of the overtopping threshold h_t appears to have a negligible influence on CW_I .

As far as the capture width ratio of the overtopping component of the device, CW_{II} (Figure 6), is concerned, maximum values of about 0.08 are obtained in the tested range of conditions. The maximum CW_{II} corresponds to the O^2WC configuration having $G/H = 1.5$, intermediate overtopping threshold height ht_2 and relative water depth $kh = 1.14$ (Figure 6d). It is worth noting that the higher kh -values tested ($kh = 2.41$ and $kh = 1.75$, Figure 6a,b) are associated with null CW_{II} , since as aforementioned in such conditions the submerged connection between the two chambers is located too deep underwater for transmitting relevant wave-induced effects to the overtopping chamber.

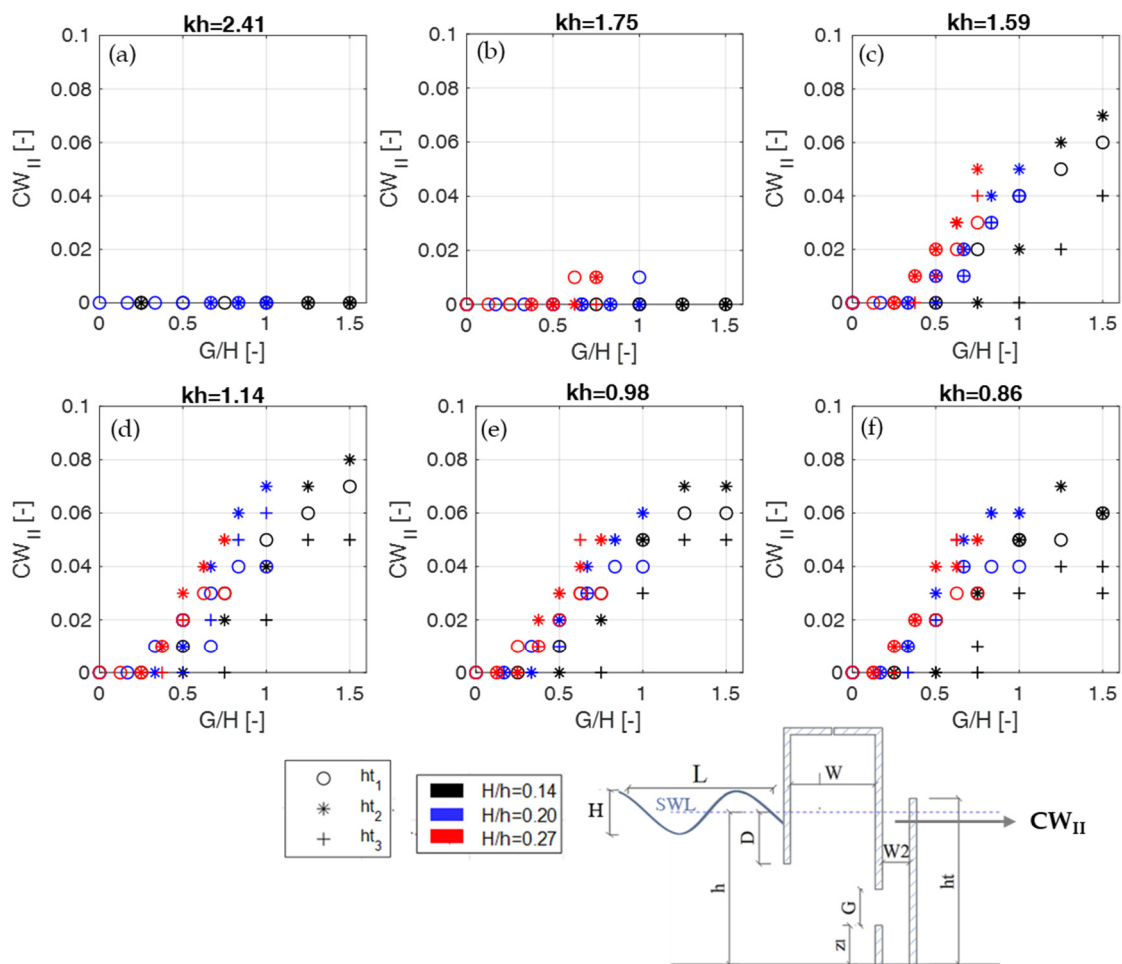


Figure 6. Capture width of the overtopping-based component of the device, CW_{II} , as a function of the relative size of the submerged aperture G/H (where G is the size of the back-wall gap and H is the incident wave height) for different relative water depths: $kh = 2.41$ (a), 1.75 (b), 1.59 (c), 1.14 (d), 0.98 (e), 0.86 (f).

For $kh < 1.59$, CW_{II} shows an increasing trend with G/H . The higher CW_{II} values are obtained for the smallest incident wave height H/h : for $kh = 1.14$, e.g., the maximum

CW_{II} attained for the highest wave ($H/h = 0.27$) is about 0.05, while for the smallest wave ($H/h = 0.14$) a higher $CW_{II} = 0.08$ is achieved.

Further increasing kh to values < 1.14 (Figure 6d–f), rising G/H to values higher than 1 does not result in significant increases in CW_{II} .

The different functional dependence between CW_{II} and G/H observed for different kh may be physically interpreted as the results of a balance between the phenomena through which the position and the size of the connection between the two chambers affect the water column motion. From one side, the resonance frequency of the OTD chamber is shifted towards higher values (i.e., towards higher kh values on a fixed water depth h) for a larger size of the aperture G . Indeed, increasing G implies reducing the draft of the oscillating water column in the OTD chamber, therefore it directly affects the resonance frequency. On the other side, as aforementioned, increasing G also means locating the aperture at a lower depth below the water, therefore increasing the wave excitation on the OTD chamber. The balance of these two phenomena determines the shape of the functional dependence of the oscillation amplitude on G for different kh (in turn determining q_{otd} and CW_{II}).

3.1.2. Effect of the Relative Chamber Width W/L

The capture width CW_I as a function of the relative width of the OWC chamber, W/L , for different apertures of the submerged gap G , is reported in Figure 7. For the sake of readability, only results obtained with the smallest incident wave height H/h are included in Figure 7. For the O²WC configuration resembling a traditional OWC, i.e., that with the back wall completely closed ($G = 0$, Figure 7a), CW_I attains the higher values (about 0.7) for $0.1 < W/L < 0.15$. Such a result is consistent with previous studies in the literature on the optimization of the geometry for traditional OWC converters [17]. As discussed in Section 3.1.1, progressively increasing the size of the submerged aperture, CW_I decreases, particularly in the lower range of W/L (i.e., for the longer incident wavelengths, since W is kept constant in the present study). The shape of the functional dependency between CW_I and W/L is, therefore, progressively modified, with the maximum CW_I shifting towards higher W/L values: for $0.75 < G/H < 1.5$ (Figure 7d–g), CW_I peaks for approximately $W/L = 0.16$, attaining a maximum of 0.53 for the smallest incident wave height $H/h = 0.14$. In the range $0.1 < W/L < 0.15$, instead, higher G/H values result in substantial decrease of CW_I , which reaches, respectively, a maximum of: 0.4 for $G/H = 0.75$ (Figure 7d), 0.35 for $G/H = 1$ (Figure 7e) and 0.3 for $G/H = 1.25$ – 1.5 (Figure 7f,g). For $W/L > 0.2$, CW_I was found to be lower than 0.15, irrespective of the value of the relative gap size G/H and the relative wave height H/h .

Within the investigated range of parameters, the second component of the device capture width CW_{II} as a function of W/L (Figure 8) exhibits maximum values for W/L around 0.1, i.e. close to the values maximizing also CW_I . For $W/L > 0.1$, CW_{II} rapidly decreases for all the tested sizes of the back wall aperture G/H , up to zeroing for $W/L > 0.15$, regardless of the value of the overtopping threshold height ht adopted and that of the aperture in the OWC chamber back wall. Qualitatively similar results are obtained with the highest incident waves $H/h = 0.20$ and $H/h = 0.27$, as reported in Appendix A.

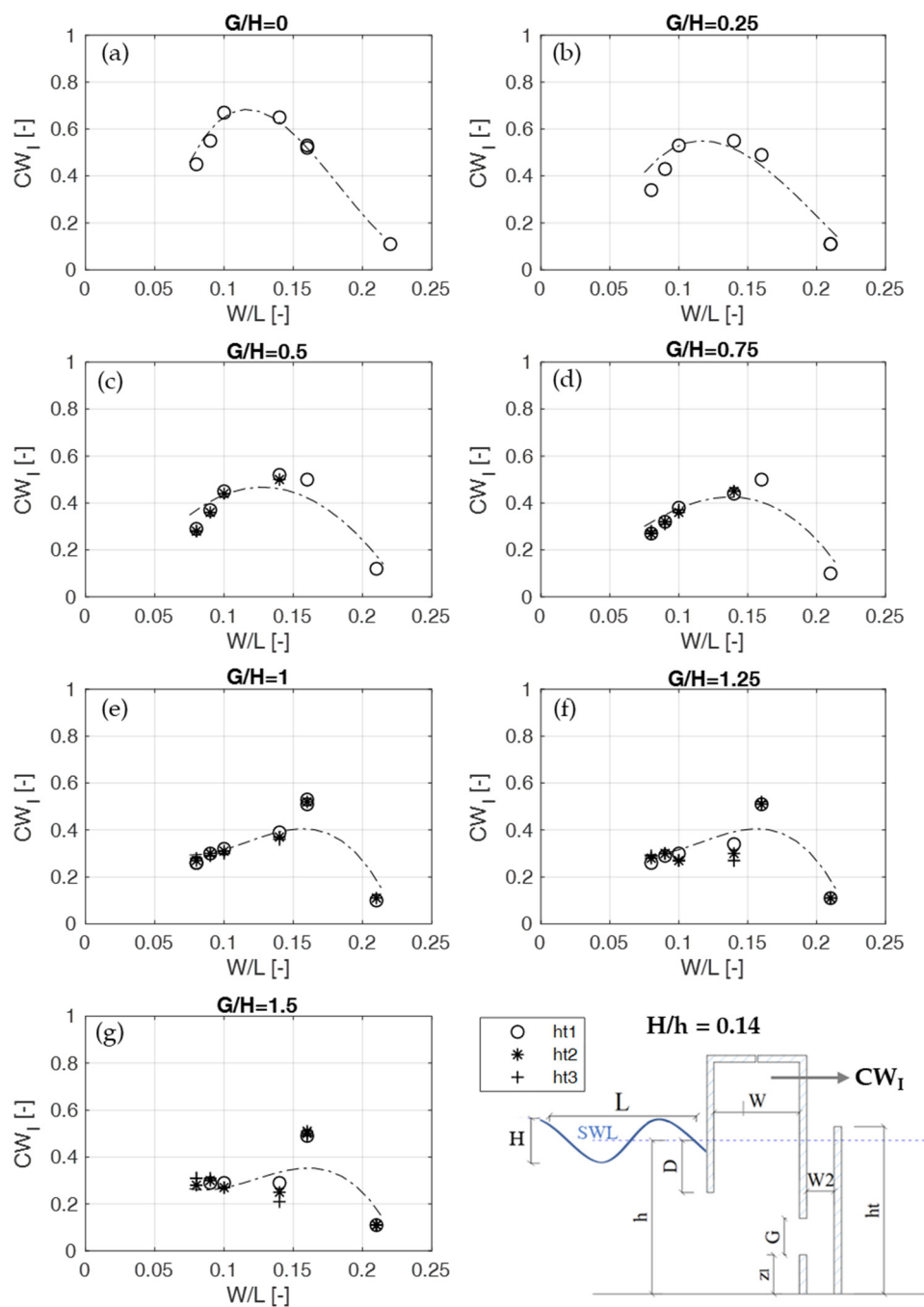


Figure 7. Capture width of the OWC chamber CW_I as a function of the relative width of the OWC chamber, W/L , for different sizes of the aperture in the back wall relative to the water depth h : $G/H = 0$ (a), 0.25 (b), 0.5 (c), 0.75 (d), 1 (e), 1.25 (f), 1.5 (g). Results are obtained for $H/h = 0.14$.

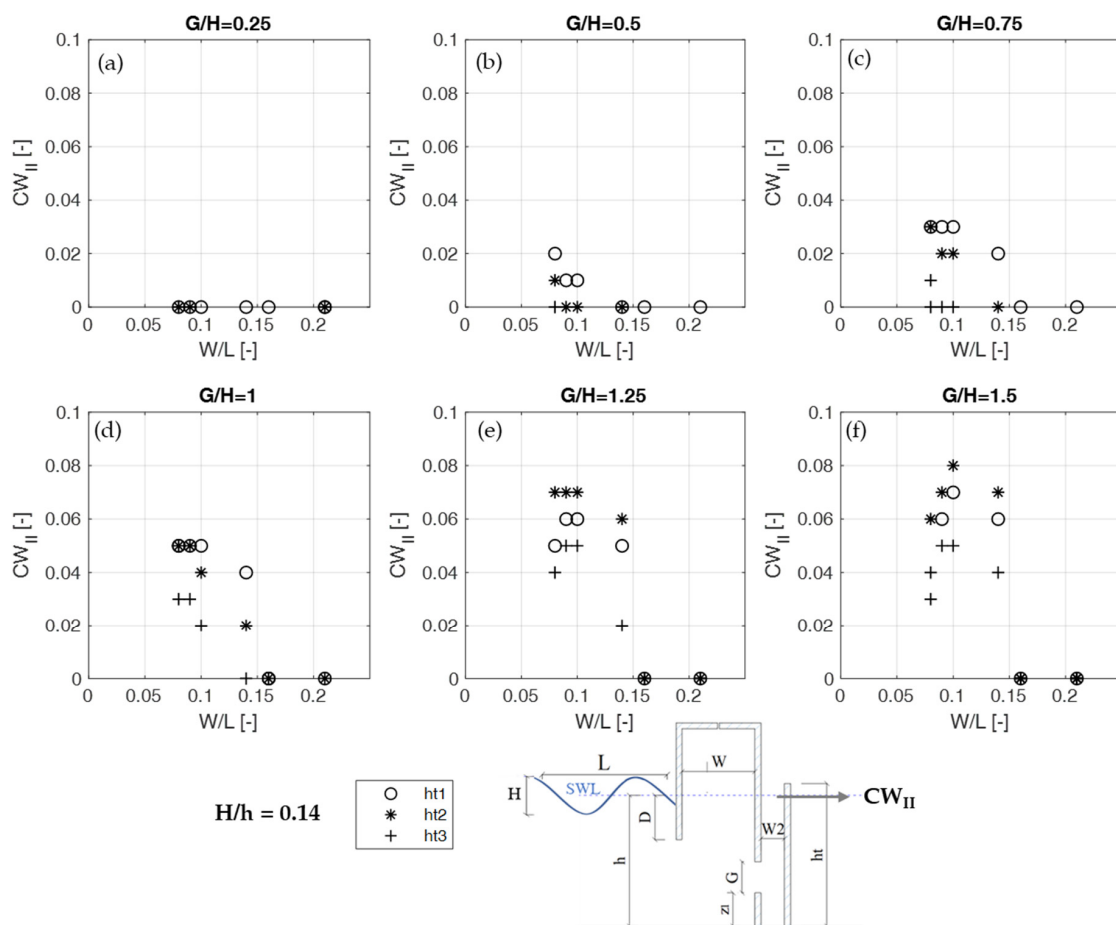


Figure 8. Capture width of the overtopping-based component of the device, CW_{II} , as a function of the width of the OWC chamber, W/L , for different sizes of the aperture in the back wall relative to the incident wave height $G/H = 0.25$ (a), 0.5 (b), 0.75 (c), 1 (d), 1.25 (e), 1.5 (f). Results are obtained for $H/h = 0.14$.

3.1.3. Effect of the Overtopping Threshold Height ht

The overtopping threshold height ht , has a fundamental effect on the performance of the overtopping chamber CW_{II} , directly determining both the overtopping rate q_{otd} and the available hydraulic head Δh_{otd} to be converted by the turbine.

The highest CW_{II} is obtained for the intermediate value of the overtopping threshold height ht_2 (for configuration $G/H = 1.5$, $W/L = 0.1$, $H/h = 0.14$). Also for the other configurations, for fixed values of the other design parameters, the intermediate threshold ht_2 allows obtaining higher CW_{II} in most of the tested cases. Therefore, the optimum height of the overtopping threshold, in terms of maximization of the capture width of the overtopping-based component of the device, appears to be contained within the investigated range of ht values.

For the smallest incident wave height considered in this study ($H/h = 0.14$, Figure 8), fixing G/H and W/L , the intermediate height of the overtopping threshold ht_2 gives higher CW_{II} than the lowest threshold ht_1 for high gap apertures G/H (i.e., $G/H = 1.25$ and $G/H = 1.5$, Figure 8e,f). Instead, for intermediate G/H values ($G/H = 0.5$ – 1 , Figure 8b–d), higher CW_{II} is obtained with ht_1 . In such conditions, the lower wave energy transmission through the smaller submerged gap, with the consequent smaller oscillation amplitude in the second chamber, shifts the optimal working configuration towards that comprising the reduced hydraulic head and the higher overtopping rates obtained with the lower threshold ht . This trend towards a decrease of the optimal overtopping threshold height for

decreasing G/H takes place regardless of the value of the relative chamber width W/L , i.e., it is quite insensitive to the incident wavelength.

Similarly, when considering higher incident waves ($H/h = 0.2$ and $H/h = 0.27$, as reported in Figures A1 and A2 of Appendix A), the intermediate threshold ht_2 allows achieving the highest CW_{II} under most of the geometry and wave conditions tested. For the greater level of the aperture of the gap G , however, similar wave energy conversion performances are obtained also with the highest threshold ht_3 .

The processes in the OWC chamber both in terms of CW_I and maximum air pressure) are relatively unaffected by the value of ht (Figures 7 and 9).

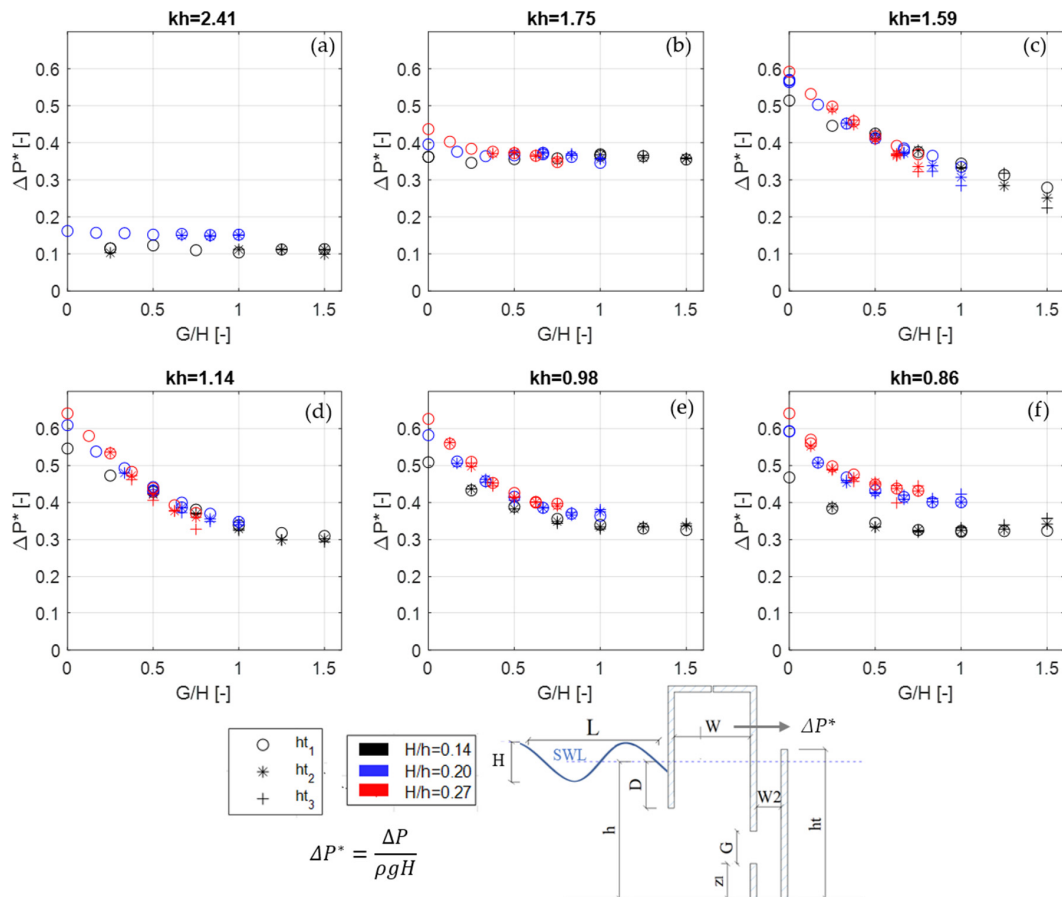


Figure 9. Dimensionless pressure parameter ΔP^* as a function of the relative size of the submerged aperture G/H for different relative water depths: $kh = 2.41$ (a), 1.75 (b), 1.59 (c), 1.14 (d), 0.98 (e), 0.86 (f).

3.2. Air Pressure Inside the OWC Chamber

To analyse the capability of the O^2WC concept in reducing the maximum air pressure in the primary OWC chamber, the dimensionless pressure parameter ΔP^* , defined as in Equation (5), is introduced.

$$\Delta P^* = \frac{\Delta P}{\rho g H} \tag{5}$$

where ΔP is the height of the air pressure oscillation in the OWC chamber, ρ is the water and H is the incident wave height.

When considering the parameter ΔP^* , the relative water depth kh affects the response of the O^2WC system to variations in the size of the gap in the back wall G/H . Figure 9 represents the variation of ΔP^* as a function of G/H , for different relative water depth kh and incident wave heights.

Varying the configuration from the classical OWC device (i.e., $G/H = 0$) to that of the O^2WC with progressively higher values of the gap in the back wall (i.e., for G/H increasing

up to 1.5), ΔP^* does not show significant variations in the higher kh range ($kh = 2.41$ and 1.75 , Figure 9a,b). As aforementioned, under such conditions, the submerged aperture is located too deep underwater to transmit relevant wave-induced to the overtopping chamber.

As expected from the previously examined trends in CW_I , for $kh > 1.75$, increasing G/H -values are associated with decreasing pressure in the OWC chamber ΔP^* . For $kh = 1.59$, an approximately linear decreasing trend of ΔP^* with G/H is observed (Figure 9c). Further increasing kh , instead, the rate of decrease of ΔP^* with G/H is no longer constant over the explored range of parameters. Indeed, ΔP^* tends to become quite insensitive to G/H for values >0.75 . As an example, for $kh = 1.14$ and $H/h = 0.14$ (Figure 9d), ΔP^* decreases as follows: (i) from 0.55 to 0.35 (with a relative decrease of 36%) for G/H increasing from 0 to 0.75; (ii) from 0.35 to 0.3 (relative decrease of 14%) for the further increase of G/H from 0.75 to 1.

4. Discussion

In the case of a conventional OWC device (O^2WC configuration with the back wall completely closed, $G = 0$), a maximum value of $CW_I = 0.7$ is obtained in the present study. Such value is consistent with previous studies on the OWC performance [15–17]. As far as the OTD chamber is concerned, also the values obtained for CW_{II} (reaching a maximum of 0.08) are in line with the available references on conventional OTD-WECs, for which capture width values ranging between 0.1 and 0.3 are documented [12,28]. As a further comparison, it is worth mentioning that the hybrid device MoonWEC [13], proposed specifically for wave power extraction in the Mediterranean Sea combining the principles of the heaving point absorber, the oscillating water column and the overtopping, shows maximum CW -values up to 0.9, with average values over the sea-states of specific installation locations in Italy of about 0.4–0.45. Including the performance of a linear generator, the point absorber WEC proposed by Bozzi et al. [6] shows CW values up to 0.4 for the hypothetical installation off the Alghero coast (Italy), with maximum conversion performance for sea states with peak period between 3–4 s, decreasing to $CW < 0.15$ for peak periods higher than 6 s. The power extraction potential of the O^2WC seems, therefore, in line with that of other devices proposed for exploiting Mediterranean Sea waves.

For the specific case of the O^2WC device, in the perspective of maximizing CW_{II} , data analysis revealed that an optimal value of the height of the overtopping threshold from the OTD chamber ht can be individuated within the studied parameter range. Indeed, the intermediate overtopping threshold ht_2 allows maximizing CW_{II} for most of the incident wave height and periods. The amplitude of the water oscillation inside the OTD chamber, and therefore the overtopping discharge for a fixed value of the overtopping threshold ht , is a function of both the natural resonance frequency of the OTD chamber and of the dynamic wave forces acting at the level of the submerged aperture. Therefore, further possibilities for increasing CW_{II} consist in optimizing the vertical position of the aperture connecting the two chambers (in this work fixed at z_1 height above the bottom, as in Table 1), regulating both the aforementioned factors (i.e., resonance and wave-induced loads on the water column in the OTD chamber). Worth to note that a detailed background on the resonance frequency for WEC based on oscillating systems can be found, e.g., in [44,45]. From physical arguments, such concepts may be extended to represent also the resonance frequency of the water column in the OTD chamber.

Compared to a conventional OWC device, the O^2WC concept has been proven to be capable of decreasing the pressure oscillation amplitude ΔP^* in the OWC chamber (as discussed in Section 3.2 and Figure 9), possibly promoting safer operability of the air turbine in highly energetic sea states. It is worth highlighting that such a decrease in the air pressure oscillation amplitude in the OWC chamber corresponds to an equivalent decrease in the primary conversion efficiency of the OWC component of the device CW_I (as observed in Section 3.1), which is only partially compensated by the additional CW_{II} obtained by accumulating the potential energy of the overtopped water flow in the second chamber. As an example, for the relative water depth $kh = 1.14$, the performance of a pure OWC device

($G/H = 0$) attains a value of $CW = \sim 0.7$, while considering the O^2WC concept with a relative gap size $G/H = 0.75$, the OWC chamber has a $CW_I = 0.4$. An additional $CW_{II} = 0.06$ is recovered in the OTD chamber, therefore the O^2WC has a total $CW = 0.46$, i.e., 24 percentage points lower than that of the pure OWC. In this configuration, the pressure oscillation amplitude ΔP^* in the OWC chamber has a relative reduction of about 39% regarding the pure OWC case.

To provide a complete assessment of the performance of energy extraction of the device, beyond the primary conversion efficiency, which is studied in this work, the testing of the performance of the whole energy conversion chain from waves to electrical wire (wave-to-wire) should be performed (as presented e.g., in [46,47]). In this respect, the aerodynamic performance of the air turbine plays a major role.

Air turbines for OWC, and Wells turbine in particular, may have limited operability in highly energetic wave conditions due to excessive centrifugal stresses [20]. Moreover, Wells turbines are also particularly prone to a stall-related sharp loss of efficiency when the flow rate overcomes a certain limit, which depends on the aerodynamic characteristics of the turbine and on its rotational speed [14]. Both the aforementioned phenomena are fundamentally turbine-specific [20,21]. Therefore, specifying the maximum operative pressure allowable in the air chamber of an OWC device is far from trivial. Indeed, the problem can't be decoupled from the knowledge of the specific turbine with should operate in the given device.

Moreover, the frequency of occurrence of the most energetic sea states in which survival measures (e.g., closing a valve in series with the turbine, or opening a bypass valve to limit the air pressure) should be adopted is supposed to be relatively small compared to the operative wave conditions, possibly limiting the usefulness of adopting the O^2WC concept. Therefore, an evaluation of the relative gains obtained by using the O^2WC should be carried out by comparatively assessing the performance of the device, from wave-to-wire, under the wave conditions of a reference installation site, considering the average power output on an annual basis.

It is finally worth mentioning that the additional construction costs, compared to a classical breakwater integrated OWC, due to the need of realizing a double chamber device and installing two PTO systems, as well as the impact on the overall LCOE, should be carefully evaluated in more advanced stages of the device design. It is also foreseen that, although characterized by lower pressure than a classical OWC, the O^2WC device would still have to be equipped with extra safety valves to protect the integrity of the mechanical parts under the most extreme wave actions.

5. Conclusions

In this paper, the wave energy conversion performance and capability to reduce the maximum air chamber pressure in the O^2WC device have been presented. The O^2WC is a hybrid concept between the OWC and the OTD technologies, particularly suited for bottom-standing breakwater integration. The study is based on a laboratory test campaign carried out on a 1:25 scaled model.

The performance of the device has been investigated under different incident wave conditions, evaluating the effect of a set of geometrical parameters (size of the opening hydraulically connecting the OWC and OTD chambers, height of the overtopping threshold in the second chamber).

The maximum capture width CW of the OWC chamber reached a value of around 0.7 in the pure OWC configuration, while the OTD component attained a maximum CW of 0.08. Data analysis revealed that, among the tested geometry alternatives, an optimal value of the height of the overtopping threshold from the second chamber of the device can be detected to maximize the wave energy conversion capability of the overtopping-based component of the system. Further improvements in the conversion performance of the O^2WC could be achieved by optimizing the depth of the aperture connecting the two chambers, which influences the resonance frequency of the water column in the OTD chamber.

The presented results show that, in the O^2WC , the hydraulic connection between the OWC and the OTD chambers allows reducing the maximum air pressure and airflow rates in the OWC chamber. In this way, it could be possible to implement strategies for the safe functioning of the air turbine under extreme conditions and to extend the operative range of the device, while storing in the form of potential energy in the OTD chamber part of the energy that would be alternatively dissipated employing relief valves. However, it must be highlighted that the decrease of the air pressure oscillation amplitude (and, correspondingly, of water level oscillation and air flow rates) in the OWC chamber results in an equivalent decrease in the primary conversion efficiency of the OWC component of the device, under both operative and extreme wave conditions. Such a decrease in efficiency can be only partially compensated by the additional wave energy conversion process taking place in the OTD component of the O^2WC .

Further analyses, comprising a wave-to-wire modelling of the O^2WC which includes the air turbine aerodynamics, are fundamental for evaluating the range of conditions in which the proposed concept could effectively offer advantages compared to a classical OWC. Laboratory data acquired in the presented test campaign could be used to validate numerical models aimed at performing a finer geometry optimization of the O^2WC device.

Author Contributions: Conceptualization, L.C.; Data curation, I.S., A.E. and L.C.; Formal analysis, I.S.; Funding acquisition, L.C.; Investigation, I.S., A.E. and L.C.; Methodology, I.S. and L.C.; Writing—original draft, I.S.; Writing—review & editing, I.S. and L.C. All authors have read and agreed to the published version of the manuscript.

Funding: This research received no external funding.

Data Availability Statement: The data presented in this study are available on request from the corresponding author.

Conflicts of Interest: The authors declare no conflict of interest.

Appendix A. CWII as a Function of W/L for Additional Incident Wave Heights

Figures A1 and A2 show the capture width CW_{II} of the OTD-based component of the O^2WC as a function of the relative width of the OWC chamber, W/L , for different apertures of the submerged gap G/H , respectively for $H/h = 0.2$ and $H/h = 0.27$.

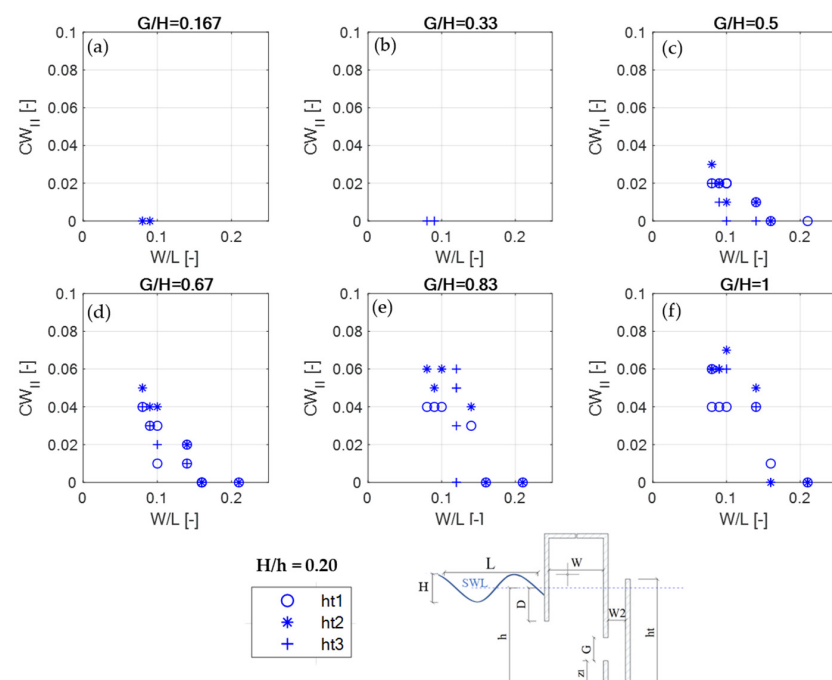


Figure A1. Capture width of the overtopping-based component of the device, CW_{II} , as a function of

the width of the OWC chamber, W/L , for different sizes of the aperture in the back wall relative to the incident wave height $G/H = 0.125$ (a), 0.25 (b), 0.375 (c), 0.5 (d), 0.625 (e), 0.75 (f). Results obtained with the wave height $H/h = 0.20$.

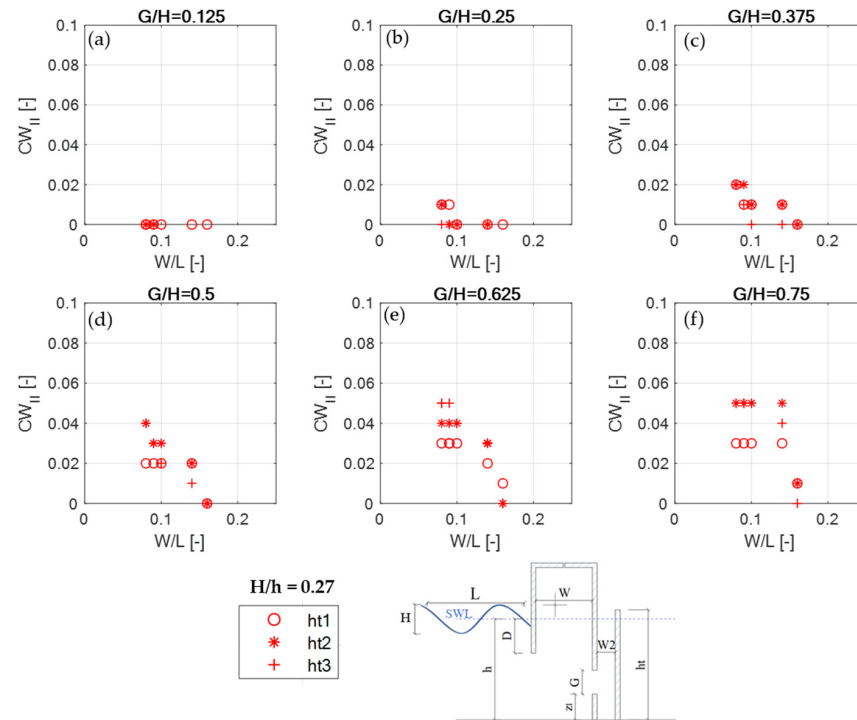


Figure A2. Capture width of the overtopping-based component of the device, CW_{II} , as a function of the width of the OWC chamber, W/L , for different sizes of the aperture in the back wall relative to the incident wave height $G/H = 0.167$ (a), 0.33 (b), 0.5 (c), 0.67 (d), 0.83 (e), 0.1 (f). Results obtained with the wave height $H/h = 0.27$.

References

1. Aderinto, T.; Li, H. Ocean Wave Energy Converters: Status and Challenges. *Energies* **2018**, *11*, 1250. [[CrossRef](#)]
2. European Commission. Directorate General for Research and Innovation, ECORYS, and Fraunhofer. In *Study on Lessons for Ocean Energy Development*; Publications Office of the European Union: Luxembourg, UK, 2017. Available online: <https://data.europa.eu/doi/10.2777/389418> (accessed on 26 September 2022).
3. Chang, G.; Jones, C.A.; Roberts, J.D.; Neary, V.S. A comprehensive evaluation of factors affecting the levelized cost of wave energy conversion projects. *Renew. Energy* **2018**, *127*, 344–354. [[CrossRef](#)]
4. Soukissian, T.; Denaxa, D.; Karathanasi, F.; Prospathopoulos, A.; Sarantakos, K.; Iona, A.; Georgantas, K.; Mavrakos, S. Marine Renewable Energy in the Mediterranean Sea: Status and Perspectives. *Energies* **2017**, *10*, 1512. [[CrossRef](#)]
5. Astariz, S.; Iglesias, G. The economics of wave energy: A review. *Renew. Sustain. Energy Rev.* **2015**, *45*, 397–408. [[CrossRef](#)]
6. Bozzi, S.; Miquel, A.M.; Scarpa, F.; Antonini, A.; Archetti, R.; Passoni, G.; Gruosso, G. Wave energy production in Italian offshore: Preliminary design of a point absorber with tubular linear generator. In Proceedings of the 2013 International Conference on Clean Electrical Power (ICCEP), Alghero, Italy, 11 June 2013; pp. 203–208. [[CrossRef](#)]
7. Bozzi, S.; Archetti, R.; Passoni, G. Wave electricity production in Italian offshore: A preliminary investigation. *Renew. Energy* **2014**, *62*, 407–416. [[CrossRef](#)]
8. Vannucchi, V.; Cappiotti, L. Wave Energy Assessment and Performance Estimation of State of the Art Wave Energy Converters in Italian Hotspots. *Sustainability* **2016**, *8*, 1300. [[CrossRef](#)]
9. Re, C.L.; Manno, G.; Basile, M.; Ciruolo, G. The opportunity of using wave energy converters in a Mediterranean hot spot. *Renew. Energy* **2022**, *196*, 1095–1114. [[CrossRef](#)]
10. Aristodemo, F.; Ferraro, D.A. Feasibility of WEC installations for domestic and public electrical supplies: A case study off the Calabrian coast. *Renew. Energy* **2018**, *121*, 261–285. [[CrossRef](#)]
11. Cappiotti, L.; Simonetti, I.; Penchev, V.; Penchev, P. Laboratory tests on an original wave energy converter combining oscillating water column and overtopping devices. In Proceedings of the 3rd International Conference on Renewable Energies Offshore (RENEW-2018), Lisbon, Portugal, 18 September 2018; p. 6.

12. Cabral, T.; Clemente, D.; Rosa-Santos, P.; Taveira-Pinto, F.; Morais, T.; Belga, F.; Cestaro, H. Performance Assessment of a Hybrid Wave Energy Converter Integrated into a Harbor Breakwater. *Energies* **2020**, *13*, 236. [[CrossRef](#)]
13. Miquel, A.; Lamberti, A.; Antonini, A.; Archetti, R. The MoonWEC, a new technology for wave energy conversion in the Mediterranean Sea. *Ocean Eng.* **2020**, *217*, 107958. [[CrossRef](#)]
14. Falcão, A.F.O.; Henriques, J.C.C. Oscillating-water-column wave energy converters and air turbines: A review. *Renew. Energy* **2016**, *85*, 1391–1424. [[CrossRef](#)]
15. Boccotti, P.; Filianoti, P.; Fiamma, V.; Arena, F. Caisson breakwaters embodying an OWC with a small opening—Part II: A small-scale field experiment. *Ocean Eng.* **2007**, *34*, 820–841. [[CrossRef](#)]
16. Morris-Thomas, M.T.; Irvin, R.J.; Thiagarajan, K.P. An Investigation into the Hydrodynamic Efficiency of an Oscillating Water Column. *J. Offshore Mech. Arct. Eng.* **2007**, *129*, 273–278. [[CrossRef](#)]
17. Simonetti, I.; Cappiotti, L.; Elsafti, H.; Oumeraci, H. Optimization of the geometry and the turbine induced damping for fixed detached and asymmetric OWC devices: A numerical study. *Energy* **2017**, *139*, 1197–1209. [[CrossRef](#)]
18. Simonetti, I.; Cappiotti, L.; Oumeraci, H. An empirical model as a supporting tool to optimize the main design parameters of a stationary oscillating water column wave energy converter. *Appl. Energy* **2018**, *231*, 1205–1215. [[CrossRef](#)]
19. López, I.; Carballo, R.; Iglesias, G. Site-specific wave energy conversion performance of an oscillating water column device. *Energy Convers. Manag.* **2019**, *195*, 457–465. [[CrossRef](#)]
20. Falcão, A.F.O.; Henriques, J.C.C.; Gato, L.M.C. Air turbine optimization for a bottom-standing oscillating-water-column wave energy converter. *J. Ocean Eng. Mar. Energy* **2016**, *2*, 459–472. [[CrossRef](#)]
21. Falcão, A.F.O.; Henriques, J.C.C.; Gato, L.M.C. Self-rectifying air turbines for wave energy conversion: A comparative analysis. *Renew. Sustain. Energy Rev.* **2018**, *91*, 1231–1241. [[CrossRef](#)]
22. Falcão, A.F.O.; Justino, P. OWC wave energy devices with air flow control. *Ocean Eng.* **1999**, *26*, 1275–1295. [[CrossRef](#)]
23. Falcão, A.F.O.; Vieira, L.C.; Justino, P.A.P.; André, J.M.C.S. By-Pass Air-Valve Control of an OWC Wave Power Plant. *J. Offshore Mech. Arct. Eng.* **2003**, *125*, 205–210. [[CrossRef](#)]
24. Faÿ, F.-X.; Henriques, J.C.C.; Kelly, J.; Mueller, M.; Abusara, M.; Sheng, W.; Marcos, M. Comparative assessment of control strategies for the biradial turbine in the Mutriku OWC plant. *Renew. Energy* **2020**, *146*, 2766–2784. [[CrossRef](#)]
25. Henriques, J.C.C.; Gomes, R.; Gato, L.M.C.; Falcão, A.F.O.; Robles, E.; Ceballos, S. Testing and control of a power take-off system for an oscillating-water-column wave energy converter. *Renew. Energy* **2016**, *85*, 714–724. [[CrossRef](#)]
26. Kofoed, J.P.; Frigaard, P.; Friis-Madsen, E.; Sørensen, H.C. Prototype testing of the wave energy converter wave dragon. *Renew. Energy* **2006**, *31*, 181–189. [[CrossRef](#)]
27. Contestabile, P.; Crispino, G.; Di Lauro, E.; Ferrante, V.; Gisonni, C.; Vicinanza, D. Overtopping breakwater for wave Energy Conversion: Review of state of art, recent advancements and what lies ahead. *Renew. Energy* **2020**, *147*, 705–718. [[CrossRef](#)]
28. Musa, M.A.; Maliki, A.Y.; Ahmad, M.F.; Yaakob, O.; Samo, K.; Ibrahim, M.Z. Prediction of Energy Performance by Adopting Overtopping Breakwater for Energy Conversion (OBREC) Concept in Malaysia Waters. *J. Environ. Sci. Technol.* **2016**, *9*, 417–426. [[CrossRef](#)]
29. Ibarra-Berastegi, G.; Sáenz, J.; Ulazia, A.; Serras, P.; Esnaola, G.; Garcia-Soto, C. Electricity production, capacity factor, and plant efficiency index at the Mutriku wave farm (2014–2016). *Ocean Eng.* **2018**, *147*, 20–29. [[CrossRef](#)]
30. Arena, F.; Romolo, A.; Malara, G.; Fiamma, V.; Laface, V. The First Full Operative U-OWC Plants in the Port of Civitavecchia. In Proceedings of the ASME International Conference on Offshore Mechanics and Arctic Engineering, Trondheim, Norway, 25–30 June 2017; Volume 10. [[CrossRef](#)]
31. Vicinanza, D.; Contestabile, P.; Nørgaard, J.Q.H.; Andersen, T.L. Innovative rubble mound breakwaters for overtopping wave energy conversion. *Coast. Eng.* **2014**, *88*, 154–170. [[CrossRef](#)]
32. Di Lauro, E.; Maza, M.; Lara, J.L.; Losada, I.J.; Contestabile, P.; Vicinanza, D. Advantages of an innovative vertical breakwater with an overtopping wave energy converter. *Coast. Eng.* **2020**, *159*, 103713. [[CrossRef](#)]
33. Palma, G.; Contestabile, P.; Zanuttigh, B.; Formentin, S.M.; Vicinanza, D. Integrated assessment of the hydraulic and structural performance of the OBREC device in the Gulf of Naples, Italy. *Appl. Ocean Res.* **2020**, *101*, 102217. [[CrossRef](#)]
34. Kralli, V.-E.; Theodossiou, N.; Karambas, T. Optimal Design of Overtopping Breakwater for Energy Conversion (OBREC) Systems Using the Harmony Search Algorithm. *Front. Energy Res.* **2019**, *7*, 80. [[CrossRef](#)]
35. Calheiros-Cabral, T.; Clemente, D.; Rosa-Santos, P.; Taveira-Pinto, F.; Ramos, V.; Morais, T.; Cestaro, H. Evaluation of the annual electricity production of a hybrid breakwater-integrated wave energy converter. *Energy* **2020**, *213*, 118845. [[CrossRef](#)]
36. Koutrouveli, T.; Di Lauro, E.; das Neves, L.; Calheiros-Cabral, T.; Rosa-Santos, P.; Taveira-Pinto, F. Proof of Concept of a Breakwater-Integrated Hybrid Wave Energy Converter Using a Composite Modelling Approach. *J. Mar. Sci. Eng.* **2021**, *9*, 226. [[CrossRef](#)]
37. Simonetti, I.; Crema, I.; Cappiotti, L.; Elsafti, H.; Oumeraci, H. Site-specific optimization of an OWC wave energy converter in a Mediterranean area. In Proceedings of the Renew 2016, 2nd International Conference on Renewable Energies Offshore, Lisbon, Portugal, October 2016; pp. 343–350. [[CrossRef](#)]
38. Maeda, H.; Kinoshita, T.; Masuda, K.; Kato, W. Fundamental Research on Oscillating Water Column Wave Power Absorbers. *J. Energy Resour. Technol.* **1985**, *107*, 81–86. [[CrossRef](#)]
39. Portillo, J.; Henriques, J.; Gato, L.; Falcão, A. Model tests on a floating coaxial-duct OWC wave energy converter with focus on the spring-like air compressibility effect. *Energy* **2023**, *263*, 125549. [[CrossRef](#)]

40. Elhanafi, A.; Macfarlane, G.; Fleming, A.; Leong, Z. Scaling and air compressibility effects on a three-dimensional offshore stationary OWC wave energy converter. *Appl. Energy* **2017**, *189*, 1–20. [[CrossRef](#)]
41. Simonetti, I.; Cappietti, L.; Elsafti, H.; Oumeraci, H. Evaluation of air compressibility effects on the performance of fixed OWC wave energy converters using CFD modelling. *Renew. Energy* **2018**, *119*, 741–753. [[CrossRef](#)]
42. López, I.; Carballo, R.; Taveira-Pinto, F.; Iglesias, G. Sensitivity of OWC performance to air compressibility. *Renew. Energy* **2020**, *145*, 1334–1347. [[CrossRef](#)]
43. Falcão, A.F.O.; Henriques, J.C.C.; Gomes, R.P.; Portillo, J.C. Theoretically based correction to model test results of OWC wave energy converters to account for air compressibility effect. *Renew. Energy* **2022**, *198*, 41–50. [[CrossRef](#)]
44. Falnes, J.; Kurniawan, A. *Ocean Waves and Oscillating Systems: Linear Interactions Including Wave-Energy Extraction*, 2nd ed.; Cambridge University Press: Cambridge, UK, 2020; Volume 8. [[CrossRef](#)]
45. McCormick, M.E. *Ocean Wave Energy Conversion*. Dover Publications: Mineola, NY, USA, 2007.
46. Penalba, M.; Ringwood, J.V. A Review of Wave-to-Wire Models for Wave Energy Converters. *Energies* **2016**, *9*, 506. [[CrossRef](#)]
47. Ciappi, L.; Simonetti, I.; Bianchini, A.; Cappietti, L.; Manfreda, G. Application of integrated wave-to-wire modelling for the preliminary design of oscillating water column systems for installations in moderate wave climates. *Renew. Energy* **2022**, *194*, 232–248. [[CrossRef](#)]